



HAL
open science

Experimental study of proteome halophilicity using nanoDSF: a proof of concept

Lorenzo Carre, Éric Girard, Bruno Franzetti

► **To cite this version:**

Lorenzo Carre, Éric Girard, Bruno Franzetti. Experimental study of proteome halophilicity using nanoDSF: a proof of concept. *Extremophiles*, 2021, 26 (1), 10.1007/s00792-021-01250-z . hal-03400447

HAL Id: hal-03400447

<https://hal.science/hal-03400447v1>

Submitted on 25 Oct 2021

HAL is a multi-disciplinary open access archive for the deposit and dissemination of scientific research documents, whether they are published or not. The documents may come from teaching and research institutions in France or abroad, or from public or private research centers.

L'archive ouverte pluridisciplinaire **HAL**, est destinée au dépôt et à la diffusion de documents scientifiques de niveau recherche, publiés ou non, émanant des établissements d'enseignement et de recherche français ou étrangers, des laboratoires publics ou privés.



Draft Manuscript for Review

**Experimental study of proteome halophilicity using
nanoDSF: a proof of concept**

Journal:	<i>Extremophiles</i>
Manuscript ID	EXT-21-Jun-0068.R1
Manuscript Type:	Method Paper
Date Submitted by the Author:	n/a
Complete List of Authors:	Carré, Lorenzo; Institut de Biologie Structurale, Girard, Eric; Institut de Biologie Structurale Franzetti, Bruno; Institut de Biologie Structurale
Keyword:	Halophiles, Salinity, nanoDSF, Protein stability, Haloarcula marismortui

SCHOLARONE™
Manuscripts

1 Table des matières

2	KEY-WORDS	2
3	ABSTRACT	2
4	INTRODUCTION	3
5	MATERIALS AND METHODS	5
6	CULTIVATION OF <i>H. MARISMORTUI</i> CELLS.....	5
7	PREPARATION OF PROTEOME EXTRACTS.....	5
8	MDH PROTEIN PRODUCTION AND PURIFICATION.....	5
9	CHARACTERIZATION OF <i>H. MARISMORTUI</i> PROTEOME AND MDH BY DIFFERENTIAL SCANNING FLUORIMETRY	5
10	RESULTS	6
11	DISCUSSION	7
12	CONCLUSION	10
13	ACKNOWLEDGEMENTS	11
14	FIGURES	12
15	FIGURE 1: NANODSF ANALYSIS OF <i>H. MARISMORTUI</i> CELL LYSATES AND PURIFIED MDH UPON HEATING	12
16	FIGURE 2: NANODSF ANALYSIS OF <i>H. MARISMORTUI</i> CELL LYSATES AND PURIFIED MDH UPON COOLING	13
17	FIGURE 3: STATISTICAL ANALYSIS OF <i>H. MARISMORTUI</i> PROTEOME SALT-DEPENDENCE.....	14
18	FIGURE S1: REPRODUCIBILITY OF NANODSF ANALYSIS OF <i>H. MARISMORTUI</i> CELL EXTRACTS.....	15
19	FIGURE S2: DETAILS OF NANODSF ANALYSIS OF <i>H. MARISMORTUI</i> CELL LYSATES	16
20	FIGURE S3: NANODSF ANALYSIS OF <i>E. COLI</i> CELL LYSATES UPON HEATING	17
21	REFERENCES	18

Experimental study of proteome halophilicity using nanoDSF: a proof of concept

CARRÉ Lorenzo¹, GIRARD Éric¹, FRANZETTI Bruno¹

¹ Univ Grenoble Alpes, CNRS, CEA, IBS, Grenoble, France.

nanoDSF analysis of *Halobacteria* proteome

Corresponding author: franzetti@ibs.fr

Key-words

Halophile, salinity, nanoDSF, protein stability, protein solubility, *Haloarcula marismortui*

Abstract

Adaption to environmental conditions is reflected by protein adaptation. In particular, proteins of extremophiles display distinctive traits ensuring functional, structural and dynamical properties under permanently extreme physical and chemical conditions. While it has mostly been studied with approaches focusing on specific proteins, biophysical approaches have also confirmed this link between environmental and protein adaptation at the more complex and diverse scale of the proteome. However, studies of this type remain challenging and often require large amounts of biological material.

We report here the use of nanoDSF as a tool to study proteome stability and solubility in cell lysates of the model halophilic archaeon *Haloarcula marismortui*. Notably, our results show that, as with single halophilic protein studies, proteome stability was correlated to the concentration of NaCl or KCl under which the cells were lysed and hence the proteome exposed. This work highlights that adaptation to environmental conditions can be experimentally observed at the scale of the proteome. Still, we show that the biochemical properties of single halophilic proteins can only be partially extrapolated to the whole proteome.

Introduction

In cellulo biochemical and biophysical properties of proteins result from a complex interplay of factors: temperature, pH, ionic force, water activity, interactions with other biomolecules, crowding, etc. While the cell may control some of these factors to preserve protein functions, physical and chemical conditions of the environment can drastically alter protein behaviours. In particular, in extreme environments, organisms thrive under permanent extreme conditions and their proteins face considerable physical and chemical challenge. However, it is now clear that protein adaptation is tightly associated with environmental adaptation, especially for extremophiles (Reed et al. 2013; Singh et al. 2020; Ando et al. 2021). Notably, comparative studies between homologous proteins of organisms isolated from various environments are useful for assessing the degree of adaptation of an organism to various conditions (Coquelle et al. 2010; Dick et al. 2016). However, protein traits associated with adaptation to extreme conditions and their consequences on function, stability, solubility or dynamics have mostly been shown with model enzymes which do not reflect the complexity and the diversity of the proteome.

While *in silico* approaches highlight global sequence biases in extremophiles associated with protein adaptation as revealed by *in vitro* studies of specific proteins (Kozlowski 2017; Avagyan et al. 2020; Panja et al. 2020), only few approaches have been used to experimentally assess protein adaptation at the scale of the proteome. In particular, *in vivo* neutron scattering have allowed quantitative observation of the intracellular dynamics of proteins (Zaccai 2020), further stressing the link between proteome properties, environmental adaptation and cellular fitness (Zaccai 2013) as exemplified with thermophiles and psychrophiles (Tehei et al. 2004), piezophiles (Martinez et al. 2016) and halophiles (Vauclare et al. 2015, 2020). However, this technique remains complex and requires large amounts of biological material.

Here we show that differential scanning fluorimetry (DSF), and especially label-free nanoDSF, represents a trackable approach to assess protein adaptation to environmental conditions at the scale of the proteome. This biophysical technique measures intrinsic fluorescence of tryptophan and light scattering as a proxy for, respectively, protein stability and solubility over a temperature gradient and allows experimental determination of apparent protein melting temperature (T_m). Among the many applications of nanoDSF, it has been extensively used for screening of chemical conditions (buffer and ligands) favoring protein stability or solubility, making it useful for structural studies of specific proteins (Niesen et al. 2007; Phillips and de la Peña 2011). In contrast, system-wide uses of DSF, such as thermal proteome profiling (TPP) (Savitski et al. 2014; Mateus et al. 2016; Sridharan et al. 2019), thermal proximity coaggregation (TPCA) (Tan et al. 2018) or Cellular Thermal Shift Assay (CETSA) (Tan et al. 2015; Dai et al. 2019) use full or lysed cells rather than purified proteins or complexes. However, to our knowledge, these approaches have mostly been limited to drug interaction screening and have never been used to measure general biophysical properties of a proteome. In this study, we used the model halophilic archaea *Haloarcula marismortui* to prove the usefulness of nanoDSF to highlight the link between proteome and environmental adaptations.

Halophilic microorganisms require high concentrations of salt in their environments to achieve optimal growth and thrive in hypersaline environments such as the Dead Sea, the Great Salt lake or the Lake Natron. Among them, halophilic archaea from the Halobacteria class often display the highest salt-tolerance and salt-dependency. *H. marismortui* was

1
2
3 102 isolated from the Dead Sea (Ventosa et al. 2015) and grows in media containing 1.7-5.1M NaCl
4 103 and achieve optimal growth at 3.4-3.9M (Ventosa et al. 2015). In these organisms, the outside
5 104 osmolarity of Na⁺ is mainly countered by a high intracellular accumulation of K⁺, which may
6 105 reach concentrations of 2 to above 4M while intracellular concentration of Na⁺ generally
7 106 remains below 2M. Depending on the growth conditions and on the technique used, it has
8 107 been shown that *H. marismortui* can intracellularly accumulate 1.4-5.5M K⁺ (Ginzburg et al.
9 108 1970; Jensen et al. 2015). While K⁺ is slightly more kosmotropic than Na⁺, according to
10 109 Hofmeister series, cytoplasm of these halophiles remains an extreme environment itself.

11 110 To cope with these extreme intracellular conditions, halobacterial proteins display
12 111 various traits which have been extensively studied with model proteins such as the malate
13 112 dehydrogenase (MDH) of *H. marismortui*. In comparison to their non-halophilic homologs,
14 113 halophilic proteins are overall highly negatively charged and less hydrophobic, especially at
15 114 the surface (Coquelle et al. 2010). The associated multilayered (Britton et al. 2006) solvation
16 115 shell associates water and salt ions such as Na⁺, K⁺, Cl⁻ (Bonneté et al. 1993; Madern et al.
17 116 2000b) and displays a disruption of pentagonal water networks (Talon et al. 2014), in which
18 117 fewer water molecules bind salt ions more tightly. As a result, halophilic proteins present
19 118 enhanced solubility and stability in hypersaline environments (Madern et al. 2000a; Tadeo et
20 119 al. 2009). These traits make them highly unstable in low salinity environments: most unfold
21 120 under 2-3M KCl (Eisenberg 1995; Coquelle et al. 2010). However, many proteins in
22 121 Halobacteria show a combination of properties of both halophilic and non-halophilic proteins
23 122 (Coquelle et al. 2010). In particular, DNA-binding, membrane and ribosomal proteins present
24 123 less halophilic traits (Becker et al. 2014). Therefore, one should be extremely careful when
25 124 extrapolating behavior of a single protein to all elements of the proteome.

26 125 Here we present the first proteome thermal denaturation analysis in Halobacteria
27 126 using nanoDSF.

28 127
29 128
30 129
31
32
33
34
35
36
37
38
39
40
41
42
43
44
45
46
47
48
49
50
51
52
53
54
55
56
57
58
59
60

130 Materials and methods

131

132 Cultivation of *H. marismortui* cells

133

134 *H. marismortui* was cultivated aerobically at 37°C under mild agitation. Initial stocks
135 were purchased at the DSMZ-German Collection of Microorganisms. Composition of medium
136 was 208g.L⁻¹ NaCl, 78g.L⁻¹ MgCl₂·6H₂O, 500mg.L⁻¹ CaCl₂·2H₂O, 125mg.L⁻¹ MnCl₂, 5g.L⁻¹, NaBr
137 580mg.L⁻¹, 10g.L⁻¹ yeast extract, pH adjusted to 7.5 with addition of 10M NaOH after
138 dissolution.

139 *E. coli* was cultivated was cultivated aerobically at 37°C under stronger agitation and
140 cells were pelleted in exponential phase.

141

142 Preparation of proteome extracts

143

144 2mL of a culture in mid or late exponential phase was centrifugated at 20,000 g for 15
145 minutes. Supernatant was discarded by aspiration and pellet was resuspend in 1mL of
146 solutions of various KCl or NaCl concentrations. Cells were then lysed by sonication or by
147 making them go back and forth several times through a 0.6mm diameter needle using a
148 syringe, taking advantage of the inner fragility of halobacterial cells.

149

150 MDH protein production and purification

151

152 *H. marismortui* malate dehydrogenase (MDH) enzyme was produced and purified as
153 previously described (Bonneté et al. 1994).

154

155 Characterization of *H. marismortui* proteome and MDH by differential scanning 156 fluorimetry

157

158 Cell lysates extracts were centrifugated at 20,000 g for 15 minutes and the supernatant
159 (soluble fraction of cell lysate) was loaded in Prometheus™ NT.48 capillaries. Thermal
160 denaturation curves were determined by measurements of protein intrinsic fluorescence. This
161 analysis was performed using label-free, native differential scanning fluorimetry (nanoDSF;
162 apparatus: Prometheus NT.48, NanoTemper). The tryptophan residues of the proteins in
163 proteome extracts were excited at 280 nm and the fluorescence intensity was recorded at 330
164 and 350 nm. Excitation power was set at 80 or 100%. The temperature of the measurement
165 compartment increased from 20 to 95 °C at a rate of 2°C per minute. Light scattering was also
166 measured as a way to detect aggregation events during heating. For renaturation assays, after
167 final temperature reached it immediately decreased back to 20°C at the same rate of 2°C per
168 minute.

169 *H. marismortui* MDH was diluted in various salt solutions to the same final protein
170 concentration (5ng.mL⁻¹).

171

171 Results

172

173 To investigate proteome dependency on salt in an extreme halophilic microorganism,
174 we used nanoDSF to measure the stability and aggregation state of proteins contained in
175 soluble fraction of *H. marismortui* cells lysed in various NaCl and KCl solutions. After
176 centrifugation, the supernatant was loaded in the capillaries, hence limiting the sample to the
177 fraction of the proteome that remains soluble in the corresponding salt conditions.

178 Detailed data measured by the Prometheus NT.48 (NanoTemper) are given in Fig. S1.

179 Like single protein studies with nanoDSF, as described in application notes of the
180 manufacturer (Martin et al. 2017), first derivative of ratio of 350/330nm fluorescence and first
181 derivative of light scattering were easier to interpretate and compare between salt conditions
182 than any of the other measurements (350 and 330 fluorescence respective signals, derivatives
183 or not, 350/330nm ratio, light scattering). Thus, thermal denaturation and aggregation curves
184 for the proteins contained in the capillaries were obtained. In spite of the fact that the sample
185 contained numerous types of proteins, peaks of fluorescence ratio and light scattering
186 derivatives, respectively associated with main unfolding and aggregation events, could be
187 reproducibly observed. In particular, harvesting cells at various OD₆₀₀ during the exponential
188 phase had little effect on denaturation curve shape and peak position, which was linearly
189 correlated to salt concentration, either NaCl or KCl (Fig. S2).

190 To assess dependency of peak position on biological material abundancy, the lysates
191 were diluted by various factors, while remaining in 4M KCl, and and thermal denaturation and
192 aggregation curves were compared (Fig. S3). Height of aggregation peaks was very sensitive
193 to dilution factor as no clear peak could be observed when lysates were diluted 10 times.
194 Denaturation peaks were less sensitive to dilution factor as they could still be recognized at
195 higher dilutions but with decreasing sharpness and resolution. Moreover, dilution slightly
196 shifted the horizontal position of the peak but to a lower extent than changing salt
197 concentration did in the previous experiment. Nonetheless, little difference was observed in
198 the thermal denaturation profile when with a dilution factor of 2.

199 To compare behaviour of *H. marismortui* proteome to a single halophilic protein used
200 as control, thermal denaturation and aggregation curves were obtained with both cell lysates
201 and purified MDH enzyme from the same organism (Fig. 1a and Fig. 1b). For both samples,
202 increasing concentration of NaCl or KCl delayed thermal denaturation. However, while MDH
203 of *H. marismortui* reached its peak stability at 4.0M NaCl, proteome stability continued to be
204 stabilized by higher concentrations of NaCl. In contrast, no denaturation peak could be
205 obtained with *E. coli* lysates in similar conditions, even at lowest salt concentrations (Fig. S4).

206 Unlike denaturation curves, aggregation curves presented one or two peaks of first
207 derivative of light scattering at more constant temperatures, around 70-75°C for cell lysed in
208 most conditions and always at temperatures higher than the ones associated with peak
209 denaturation event. Sharpest and most-recognizable peaks happened at high concentrations
210 of NaCl or KCl, depending on the experiment (Fig. S2) Aggregation peak at concentration of
211 salt below 3M was observed only once.

212 As with denaturation, no aggregation peak could be observed when the capillaries
213 were loaded with *E. coli* lysates under any salt concentration (Fig. S4), showing that the peaks
214 could not be a product of the salt only. Even less conditions allowed observation of
215 aggregation peaks with the purified *H. marismortui* MDH as they could only be clearly
216 observed with NaCl and at concentrations above 4.0M.

1
2
3 217
4 218 After the maximum temperature (95°C) was reached, the measurement continued
5 219 along a temperature decrease to the initial temperature (20°C) by selecting the refolding ramp
6 220 option with the aim to investigate the reversibility of the denaturation and aggregation events
7 221 observed during the heating process. The associated curves are given in Fig. 2a and Fig. 2b.
8 222 During the cooling ramp, peaks of first derivative of ratio of 350/330nm fluorescence,
9 223 putatively associated with renaturation events, were observed with both *H. marismortui* cell
10 224 lysate and MDH but only in the presence of 2.5 to 3.5M of either NaCl or KCl. In addition, these
11 225 peaks were fainter and less sharp than those observed in the denaturation curves. Moreover,
12 226 no peak of first derivative of light scattering was observed at all.

13 227 Since denaturation curves of cell lysates were more complex than those of the MDH,
14 228 we chose thereafter to compare only the proteome melting temperatures (T_{pm}), namely
15 229 temperatures associated with dominant denaturation event and peak of first derivative of
16 230 ratio of 350/330nm fluorescence. To assess reproducibility of relation between salt
17 231 concentration and T_{pm} value, we retrieved them from the 4 independent experiments shown
18 232 in Fig. S1, obtained with *H. marismortui* cells pelleted from independent cultures at various
19 233 OD₆₀₀ values. T_{pm} was plotted as a function of NaCl and KCl concentration (Fig. 3a and Fig. 3b)
20 234 and slopes of the lines fitting the data were calculated (Fig 3c). Comparing slopes rather than
21 235 T_{pm} , allowed direct comparison of dependence of thermostability on NaCl and KCl of proteins
22 236 contained in the soluble fraction of cell lysates. Results showed that T_{pm} was statistically and
23 237 significantly more dependent on KCl than NaCl and higher, at equal molarity, with KCl than
24 238 with NaCl.

25 239

26 240 Discussion

27 241
28 242 By using nanoDSF to analyze cell lysates of *H. marismortui* in various salt conditions,
29 243 we could successfully and reproducibly analyze the KCl and NaCl dependencies of stability and
30 244 solubility of the proteome. Since lysates were centrifugated prior to loading the capillaries,
31 245 the representative character of the proteome of the samples remains questionable. In
32 246 particular, proteins which were not soluble in the salt solutions, such as membrane proteins,
33 247 probably pelleted and did not contributed to the denaturation and aggregation curves. Yet,
34 248 the complexity of the curves and the linear response to the salt concentration suggest that
35 249 the capillaries contained a large portion of similar proteins of the soluble fraction the
36 250 proteome. Still, the observations could either be representative of the global protein
37 251 compositions or dominated by one or few specific proteins which would be more abundant
38 252 or would have more DSF-relevant tryptophan residues.

39 253 Since cytosol ionic composition in Halobacteria is dominated by K⁺ rather than Na⁺,
40 254 most NaCl conditions did not reflect physiological intracellular environment. However, various
41 255 studies have shown that *H. marismortui* can accumulate Na⁺ at concentrations as high as 2.6-
42 256 3.0M, depending on the growth conditions and stage (Ginzburg and Ginzburg 1976; Thombre
43 257 et al. 2016). Nonetheless, independently from the physiological likeliness of the conditions,
44 258 studying biochemical and biophysical properties of halophilic proteins in high concentrations
45 259 of ions less abundant in cytosols of Halobacteria such as Na⁺ and Mg²⁺ have revealed intriguing
46 260 effects of salt type and concentration on protein stability and solubility (Ebel et al. 2002).

47 261 Overall, our data showed that increasing salinity delayed thermal denaturation of the
48 262 *H. marismortui* proteome, which was interpreted as an expected stabilizing effect of both

1
2
3 263 NaCl and KCl. Consistent with previous studies on this single protein (Calmettes et al. 1987;
4 264 Madern and Zaccai 1997; Coquelle et al. 2010), MDH was also similarly stabilized by increasing
5 265 concentration of both NaCl and KCl. However, as indicated by the shift of the melting
6 266 temperature, MDH was more sensitive than the proteome to the increase of NaCl or KCl
7 267 concentration. Moreover, the purified enzyme reached peak stability at 4M NaCl whereas the
8 268 proteome of *H. marismortui* continued to be stabilized to the highest concentrations. In
9 269 addition, a denaturation peak could be observed when cells were lysed in deionized water
10 270 (0M salt condition) whereas the MDH showed no denaturation peak at concentrations lower
11 271 than 1M KCl or NaCl. Since MDH of *H. marismortui* has been shown to almost entirely
12 272 precipitate at such low salinities (Coquelle et al. 2010), the capillaries in the corresponding
13 273 conditions may have been loaded with less to no protein. While the cells may have released
14 274 some intracellular ions during the lysis, their dilution was too high to explain the persistence
15 275 of a proteome denaturation peak in pure water. Other explanations include the presence of
16 276 other cellular factors, such as chaperonins or small organic molecules ensuring proteome
17 277 stability in low salt conditions, or the possibility that proteins from high molecular weight
18 278 assemblies, which retain activity and hence structure in low salt conditions (Shevack et al.
19 279 1985) showing a lower sensitivity to low salinity conditions, such as ribosomes, which are less
20 280 sensitive to low salinity conditions, contributed more to the peak than in the other salt
21 281 conditions. In addition, other enzymes from *H. marismortui* are functional below 2M KCl, such
22 282 as a catalase-peroxidase (Cendrin et al. 1994), an esterase (Camacho et al. 2009), an AMP-
23 283 forming acetyl-CoA synthetase (Bräsen and Schönheit 2005) and an alkaline phosphatase
24 284 (Goldman et al. 1990).

25 285 The denaturation curves of *E. coli* lysates showed an opposite behaviour with an initial
26 286 decrease of first derivative of ratio of 350/330nm fluorescence which was followed by an
27 287 increase, even when cells were lysed in pure water (0M salt condition). However, the signal
28 288 over noise ratio was considered to be too low to propose proper explanations for such profile,
29 289 especially in comparison to the experiments with *H. marismortui*. Absence of both
30 290 denaturation and aggregation clear peaks with lysates of *E. coli* may be caused by the fact that
31 291 its proteins could denature on a wider range of temperatures, limiting the possibility of
32 292 observing define peaks.

33 293 Interpretation of the absence of aggregation peak at low salinities was even less trivial.
34 294 Indeed, aggregation curves of MDH showed no peaks below 4.0M of NaCl or at any KCl
35 295 conditions. Since proteins of halophiles are exceptionally soluble (Talon et al. 2014) and since
36 296 denaturation peaks were observed at the same time, an explanation for the absence of
37 297 aggregation peak could be that proteins, pure MDH and those in cell extract as well, remained
38 298 soluble after denaturation in low salinity conditions. However, as aggregation was dependent
39 299 on dilution factor, such explanation should be taken with caution.

40 300 The observed specific proteome behaviour could result from the fact that it contains
41 301 proteins which are less acidified than model halophilic enzymes such as the MDH. In particular,
42 302 it has been shown that protein acidification occurs to a lesser extent in various protein types:
43 303 membrane-associated proteins, subunits of large molecular weight assemblies and nucleic
44 304 acid-binding proteins, which are either excluded from the cytosolic hypersaline solvent or
45 305 interact with DNA or RNA, which are negatively charged, hence requiring positively charged
46 306 residues (Becker et al. 2014). As such, proteasome (Franzetti et al. 2002) and ribosome
47 307 (Shevack et al. 1985) of *H. marismortui* are less sensitive to low KCl concentrations than MDH.
48 308 Contribution of these proteins, especially ribosomal proteins which are among the most
49 309 abundant in many cell types (Liebermeister et al. 2014), may hence explain the differences

1
2
3 310 observed between *H. marismortui* proteome and MDH. Nonetheless, this stresses that the
4 311 behaviour of the proteome can only partially be extrapolated from that of a given enzyme.

5 312 Our experimental setup allowed little to no observation of peaks of first derivative of
6 313 ratio of 350/330nm fluorescence during the cooling step following the heating. When
7 314 observed, these renaturation peaks were less distinctive than those associated with
8 315 denaturation. Moreover, no peak of first derivative of light scattering could be observed at all,
9 316 showing that aggregation process was also mostly irreversible. Since aggregation peaks
10 317 happened after denaturation peaks during the heating step, irreversible aggregation may be
11 318 the reason why renaturation was very limited, even with the pure MDH. In the case of the
12 319 proteome, the limited renaturation could be associated with a specific subset of proteins
13 320 whose denaturation was reversible, rather than a partial renaturation of the whole proteome.
14 321 This was unlike the β -lactamase from the moderately halophilic bacterium *Chromohalobacter*
15 322 sp. 560 which has been shown to refold spontaneously after thermal denaturation in 0.2M
16 323 NaCl (Tokunaga et al. 2004). However, after being expressed in non-halophilic *Escherichia coli*
17 324 cells where it has undergone low salt denaturation, *H. marismortui* MDH can be refolded *in*
18 325 *vitro* by increasing the salinity (Cendrin et al. 1993; Franzetti et al. 2001). Similarly, a
19 326 nucleoside diphosphate kinase from the extremely halophilic archaea *H. salinarum*, which has
20 327 been expressed in *E. coli*, has also been shown to require high salt concentration for refolding
21 328 while being stable and active in low salinity conditions (Ishibashi et al. 2001), stressing the
22 329 possibility of renaturation after low salt denaturation.

23 330 However, it should be kept in mind that renaturation may be enhanced by changing
24 331 the maximum temperature reached during the cooling step. Nonetheless, salt plugs were
25 332 occasionally observed at the ends of the capillaries, presumably due to water evaporation,
26 333 hence potentially changing the salt concentrations which the samples were exposed to.
27 334 Hence, nanoDSF may not allow the proper monitoring of renaturation processes as well as
28 335 denaturation and aggregation processes for halophilic systems.

29 336
30 337 As observed with T_{pm} values and dependencies on salts, KCl was significantly more
31 338 efficient at stabilizing *H. marismortui* proteome than NaCl. While Na^+ is closer to the salting-
32 339 in and denaturing side of the Hofmeister series (Okur et al. 2017), several studies suggest
33 340 instead that K^+ is more chaotropic (Collins 1997) or less kosmotropic (Cray et al. 2013).
34 341 Nonetheless, studies on single proteins have shown contrasted effects of these salts on their
35 342 biophysical and biochemical properties.

36 343 Interestingly, neutron scattering experiments have shown that MDH of *H. marismortui*
37 344 is more resilient in NaCl than in KCl (Ebel et al. 2002), contributing to a higher stability in NaCl
38 345 than in KCl (Tehei et al. 2001, 2004). While Na^+ is more stabilizing at low salt concentrations,
39 346 little difference between the two cations on stability of MDH of *H. marismortui* was reported
40 347 at high concentrations (Zaccai et al. 1986b; Madern and Zaccai 1997). In addition, it has been
41 348 shown that this enzyme interacts with slightly more salt ions and slightly less water molecules
42 349 in NaCl than in KCl solutions (Bonneté et al. 1993). However, the requirement for salt on
43 350 stability is higher at low temperatures (Zaccai et al. 1986a; Bonneté et al. 1994). Nonetheless,
44 351 stabilisation of this enzyme in hypersaline solvents is of enthalpic nature, in contrast to the
45 352 entropic stabilization of non-halophilic BSA by salts (Tehei et al. 2001).

46 353
47 354 Moreover, it has been observed that unfolding of this enzyme was faster in low
48 355 concentrations (1M) of KCl than in NaCl (Pundak et al. 1981). Similarly, two dihydrofolate
49
50
51
52
53
54
55
56
57
58
59
60

1
2
3 356 reductases from *Haloferax volcanii* have been shown to be more stabilized by NaCl than by
4 357 KCl (Wright et al. 2002).

5 358 Concerning the enzymatic activity, various intracellular enzymes of *Haloarchaea*, such
6 359 as 3-hydroxy-3-methylglutaryl-coenzyme A reductase (Bischoff and Rodwell 1996) or NAD⁺-
7 360 dependent DNA ligase (Poidevin and MacNeill 2006), both from of *H. volcanii*, were shown to
8 361 be more active in KCl. In contrast, it has been shown that extracellular proteinases of
9 362 *Halobacterium salinarum*, which are exposed to a NaCl-rich extracellular environment, display
10 363 enhanced activity with NaCl rather than KCl (Norberg and Hofsten 1969).

11 364 Nevertheless, our results show that soluble fraction of proteome in cell lysate of the
12 365 extremely halophilic archaea *H. marismortui* does not behave identically to one of its purified
13 366 proteins and is more efficiently stabilized by KCl rather than NaCl. In contrast to the enthalpy-
14 367 dominated stabilization of its MDH, proteome of *H. marismortui* could be for example
15 368 stabilized by a combination of entropic and enthalpic effects. Because of the specificities of
16 369 each particular enzyme, the link between protein adaptation and environment adaptation
17 370 should be highlighted with global, proteome-wide approaches rather than single protein
18 371 studies.

19 372 Moreover, this work confirms that reduced proteome resilience, and presumably
20 373 lowered protein stability (Tehei et al. 2004), observed with cells of *H. salinarum* stressed with
21 374 low salt conditions (Vauclare et al. 2020) can be directly explained by the effect of lower
22 375 intracellular accumulation of KCl on proteome behaviour rather than accumulation of small
23 376 molecular weight compounds or by a change in protein expression.

377 Conclusion

378

379 In spite of the fact that nanoDSF was developed for simpler systems, salt-dependency
380 of *H. marismortui* could successfully be established and compared to those of a purified
381 enzyme from the same organism. While both were stabilized by increasing salt concentration,
382 *H. marismortui* proteome, unlike its MDH, was more efficiently stabilized by KCl, the
383 physiological intracellular salt of Halobacteria, than by NaCl, the dominant salt in most
384 hypersaline environments. Since properties of single proteins may not reflect those of the
385 global proteome from which they originate, biophysical approaches like the one proposed
386 here may help understanding the link between protein adaptation and adaptation to an
387 environment.

388 This work represents, to our knowledge, the first attempt to assess stability of large
389 fractions of the proteome of extreme halophiles using nanoDSF. This technique shows enough
390 sensitivity to observe both denaturation and aggregation peaks in such complex samples in
391 various conditions. Comparative analysis using this technique may support interpretation of
392 other biophysical measurements such as neutron scattering. Moreover, this technique could
393 be used with cell lysates from other organisms to compare their biophysical and biochemical
394 traits in relation to the physical and chemical conditions of their relative environments. In
395 particular, it may unravel specific traits at the proteome level unseen with single-protein
396 studies in thermophiles, psychrophiles, acidophiles or alkaliphiles.

1
2
3
4
5 397 **Acknowledgements**

6 398

7 399

8 400

9 401

10 402

11 403

12 404

This work is supported by the French National Research Agency in the framework of the Investissements d'Avenir program (ANR-15-IDEX-02), through the funding of the "Origin of Life" project of the Univ. Grenoble-Alpes.

IBS acknowledges integration into the Interdisciplinary Research Institute of Grenoble (IRIG, CEA).

13
14
15
16
17
18
19
20
21
22
23
24
25
26
27
28
29
30
31
32
33
34
35
36
37
38
39
40
41
42
43
44
45
46
47
48
49
50
51
52
53
54
55
56
57
58
59
60

For Peer Review

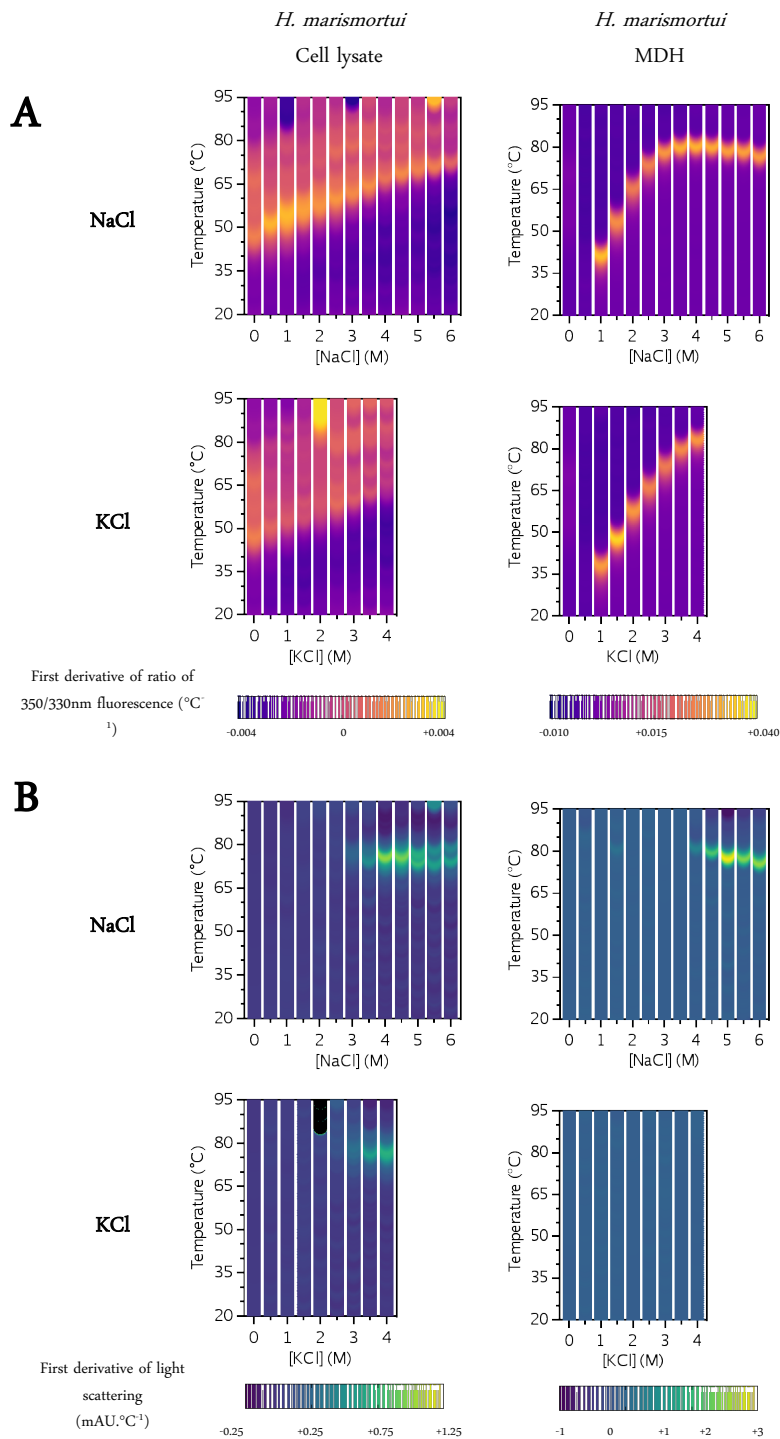
References

- 405
406
407 Ando N, Barquera B, Bartlett DH, et al (2021) The Molecular Basis for Life in Extreme
408 Environments. *Annu Rev Biophys* 50:343–372. [https://doi.org/10.1146/annurev-biophys-](https://doi.org/10.1146/annurev-biophys-100120-072804)
409 100120-072804
- 410 Avagyan S, Vasilchuk D, Makhatadze GI (2020) Protein adaptation to high hydrostatic
411 pressure: Computational analysis of the structural proteome. *Proteins: Structure, Function,*
412 *and Bioinformatics* 88:584–592. <https://doi.org/10.1002/prot.25839>
- 413 Becker EA, Seitzer PM, Tritt A, et al (2014) Phylogenetically Driven Sequencing of
414 Extremely Halophilic Archaea Reveals Strategies for Static and Dynamic Osmo-response.
415 *PLOS Genetics* 10:e1004784. <https://doi.org/10.1371/journal.pgen.1004784>
- 416 Bischoff KM, Rodwell VW (1996) 3-Hydroxy-3-methylglutaryl-coenzyme A reductase from
417 *Haloferax volcanii*: purification, characterization, and expression in *Escherichia coli*. *Journal*
418 *of Bacteriology* 178:19–23. <https://doi.org/10.1128/jb.178.1.19-23.1996>
- 419 Bonneté F, Ebel C, Zaccai G, Eisenberg H (1993) Biophysical study of halophilic malate
420 dehydrogenase in solution: revised subunit structure and solvent interactions of native and
421 recombinant enzyme. *J Chem Soc, Faraday Trans* 89:2659–2666.
422 <https://doi.org/10.1039/FT9938902659>
- 423 Bonneté F, Madern D, Zaccai G (1994) Stability against denaturation mechanisms in
424 halophilic malate dehydrogenase “adapt” to solvent conditions. *J Mol Biol* 244:436–447.
425 <https://doi.org/10.1006/jmbi.1994.1741>
- 426 Bräsen C, Schönheit P (2005) AMP-forming acetyl-CoA synthetase from the extremely
427 halophilic archaeon *Haloarcula marismortui*: purification, identification and expression of the
428 encoding gene, and phylogenetic affiliation. *Extremophiles* 9:355–365.
429 <https://doi.org/10.1007/s00792-005-0449-0>
- 430 Britton KL, Baker PJ, Fisher M, et al (2006) Analysis of protein solvent interactions in
431 glucose dehydrogenase from the extreme halophile *Haloferax mediterranei*. *PNAS* 103:4846–
432 4851. <https://doi.org/10.1073/pnas.0508854103>
- 433 Calmettes P, Eisenberg H, Zaccai G (1987) Structure of halophilic malate dehydrogenase in
434 multimolar KCl solutions from neutron scattering and ultracentrifugation. *Biophysical*
435 *Chemistry* 26:279–290. [https://doi.org/10.1016/0301-4622\(87\)80029-7](https://doi.org/10.1016/0301-4622(87)80029-7)
- 436 Camacho RM, Mateos JC, González-Reynoso O, et al (2009) Production and characterization
437 of esterase and lipase from *Haloarcula marismortui*. *Journal of Industrial Microbiology and*
438 *Biotechnology* 36:901–909. <https://doi.org/10.1007/s10295-009-0568-1>
- 439 Cendrin F, Chroboczek J, Zaccai G, et al (1993) Cloning, sequencing, and expression in
440 *Escherichia coli* of the gene coding for malate dehydrogenase of the extremely halophilic
441 archaeobacterium *Haloarcula marismortui*. *Biochemistry* 32:4308–4313.
442 <https://doi.org/10.1021/bi00067a020>
- 443 Cendrin F, Jouve HM, Gaillard J, et al (1994) Purification and properties of a halophilic
444 catalase-peroxidase from *Haloarcula marismortui*. *Biochimica et Biophysica Acta (BBA) -*
445 *Protein Structure and Molecular Enzymology* 1209:1–9. [https://doi.org/10.1016/0167-](https://doi.org/10.1016/0167-4838(94)90129-5)
446 4838(94)90129-5
- 447 Collins KD (1997) Charge density-dependent strength of hydration and biological structure.
448 *Biophysical Journal* 72:65–76. [https://doi.org/10.1016/S0006-3495\(97\)78647-8](https://doi.org/10.1016/S0006-3495(97)78647-8)
- 449 Coquelle N, Talon R, Juers DH, et al (2010) Gradual Adaptive Changes of a Protein Facing
450 High Salt Concentrations. *Journal of Molecular Biology* 404:493–505.
451 <https://doi.org/10.1016/j.jmb.2010.09.055>
- 452 Cray JA, Russell JT, Timson DJ, et al (2013) A universal measure of chaotropicity and

- 1
2
3 453 kosmotropicity. *Environmental Microbiology* 15:287–296. <https://doi.org/10.1111/1462->
4 454 2920.12018
5 455 Dai L, Prabhu N, Yu LY, et al (2019) Horizontal Cell Biology: Monitoring Global Changes of
6 456 Protein Interaction States with the Proteome-Wide Cellular Thermal Shift Assay (CETSA).
7 457 *Annu Rev Biochem* 88:383–408. <https://doi.org/10.1146/annurev-biochem-062917-012837>
8 458 Dick M, Weiergräber OH, Classen T, et al (2016) Trading off stability against activity in
9 459 extremophilic aldolases. *Scientific Reports* 6:17908. <https://doi.org/10.1038/srep17908>
10 460 Ebel C, Costenaro L, Pascu M, et al (2002) Solvent Interactions of Halophilic Malate
11 461 Dehydrogenase. *Biochemistry* 41:13234–13244. <https://doi.org/10.1021/bi0258290>
12 462 Eisenberg H (1995) Life in Unusual Environments: Progress in Understanding the Structure
13 463 and Function of Enzymes from Extreme Halophilic Bacteria. *Archives of Biochemistry and*
14 464 *Biophysics* 318:1–5. <https://doi.org/10.1006/abbi.1995.1196>
15 465 Franzetti B, Schoehn G, Ebel C, et al (2001) Characterization of a Novel Complex from
16 466 Halophilic Archaeobacteria, Which Displays Chaperone-like Activities in Vitro. *The Journal of*
17 467 *biological chemistry* 276:29906–14. <https://doi.org/10.1074/jbc.M102098200>
18 468 Franzetti B, Schoehn G, Garcia D, et al (2002) Characterization of the proteasome from the
19 469 extremely halophilic archaeon *Haloarcula marismortui*. *Archaea* 1:53–61.
20 470 <https://doi.org/10.1155/2002/601719>
21 471 Ginzburg M, Ginzburg BZ (1976) Regulation of cell volume and ion concentrations in
22 472 Halobacterium. *J Membrin Biol* 26:153–171. <https://doi.org/10.1007/BF01868871>
23 473 Ginzburg M, Sachs L, Ginzburg BZ (1970) Ion metabolism in a Halobacterium. I. Influence
24 474 of age of culture on intracellular concentrations. *J Gen Physiol* 55:187–207.
25 475 <https://doi.org/10.1085/jgp.55.2.187>
26 476 Goldman S, Hecht K, Eisenberg H, Mevarech M (1990) Extracellular Ca²⁺(+)-dependent
27 477 inducible alkaline phosphatase from extremely halophilic archaeobacterium *Haloarcula*
28 478 *marismortui*. *Journal of Bacteriology* 172:7065–7070. <https://doi.org/10.1128/jb.172.12.7065->
29 479 7070.1990
30 480 Ishibashi M, Tokunaga H, Hiratsuka K, et al (2001) NaCl-activated nucleoside diphosphate
31 481 kinase from extremely halophilic archaeon, *Halobacterium salinarum*, maintains native
32 482 conformation without salt. *FEBS Letters* 493:134–138. <https://doi.org/10.1016/S0014->
33 483 5793(01)02292-X
34 484 Jensen MW, Matlock SA, Reinheimer CH, et al (2015) Potassium stress growth
35 485 characteristics and energetics in the haloarchaeon *Haloarcula marismortui*. *Extremophiles*
36 486 19:315–325. <https://doi.org/10.1007/s00792-014-0716-z>
37 487 Kozlowski LP (2017) Proteome-pI: proteome isoelectric point database. *Nucleic Acids Res*
38 488 45:D1112–D1116. <https://doi.org/10.1093/nar/gkw978>
39 489 Liebermeister W, Noor E, Flamholz A, et al (2014) Visual account of protein investment in
40 490 cellular functions. *PNAS* 111:8488–8493. <https://doi.org/10.1073/pnas.1314810111>
41 491 Madern D, Ebel C, Mevarech M, et al (2000a) Insights into the Molecular Relationships
42 492 between Malate and Lactate Dehydrogenases: Structural and Biochemical Properties of
43 493 Monomeric and Dimeric Intermediates of a Mutant of Tetrameric l-[LDH-like] Malate
44 494 Dehydrogenase from the Halophilic Archaeon *Haloarcula marismortui*. *Biochemistry*
45 495 39:1001–1010. <https://doi.org/10.1021/bi9910023>
46 496 Madern D, Ebel C, Zaccai G (2000b) Halophilic adaptation of enzymes. *Extremophiles* 4:91–
47 497 98. <https://doi.org/10.1007/s007920050142>
48 498 Madern D, Zaccai G (1997) Stabilisation of Halophilic Malate Dehydrogenase from
49 499 *Haloarcula marismortui* by Divalent Cations. Effects of Temperature, Water Isotope,
50 500 Cofactor and pH. *Eur J Biochem* 249:607–611. <https://doi.org/10.1111/j.1432->
51 501 1033.1997.00607.x
52 502 Martin L, Schwarz S, Breitsprecher D (2017) Prometheus: the platform for analyzing protein

- 1
2
3 503 stability and thermal unfolding of proteins. 10
4 504 Martinez N, Michoud G, Cario A, et al (2016) High protein flexibility and reduced hydration
5 505 water dynamics are key pressure adaptive strategies in prokaryotes. *Sci Rep* 6:1–11.
6 506 <https://doi.org/10.1038/srep32816>
7
8 507 Mateus A, Määttä TA, Savitski MM (2016) Thermal proteome profiling: unbiased assessment
9 508 of protein state through heat-induced stability changes. *Proteome Sci* 15:1–7.
10 509 <https://doi.org/10.1186/s12953-017-0122-4>
11 510 Niesen FH, Berglund H, Vedadi M (2007) The use of differential scanning fluorimetry to
12 511 detect ligand interactions that promote protein stability. *Nat Protoc* 2:2212–2221.
13 512 <https://doi.org/10.1038/nprot.2007.321>
14 513 Norberg P, Hofsten B (1969) Proteolytic Enzymes from Extremely Halophilic Bacteria.
15 514 *Microbiology* 55:251–256. <https://doi.org/10.1099/00221287-55-2-251>
16 515 Okur HI, Hladílková J, Rembert KB, et al (2017) Beyond the Hofmeister Series: Ion-Specific
17 516 Effects on Proteins and Their Biological Functions. *J Phys Chem B* 121:1997–2014.
18 517 <https://doi.org/10.1021/acs.jpcc.6b10797>
19 518 Panja AS, Maiti S, Bandyopadhyay B (2020) Protein stability governed by its structural
20 519 plasticity is inferred by physicochemical factors and salt bridges. *Sci Rep* 10:1–9.
21 520 <https://doi.org/10.1038/s41598-020-58825-7>
22 521 Phillips K, de la Peña AH (2011) The Combined Use of the ThermoFluor Assay and ThermoQ
23 522 Analytical Software for the Determination of Protein Stability and Buffer Optimization as an
24 523 Aid in Protein Crystallization. *Current Protocols in Molecular Biology* 94:.
25 524 <https://doi.org/10.1002/0471142727.mb1028s94>
26 525 Poidevin L, MacNeill SA (2006) Biochemical characterisation of LigN, an NAD + -
27 526 dependent DNA ligase from the halophilic euryarchaeon *Haloferax volcanii* that displays
28 527 maximal in vitro activity at high salt concentrations. *BMC Molecular Biol* 7:1–14.
29 528 <https://doi.org/10.1186/1471-2199-7-44>
30 529 Pundak S, Aloni H, Eisenberg H (1981) Structure and Activity of Malate Dehydrogenase
31 530 from the Extreme Halophilic Bacteria of the Dead Sea. *European Journal of Biochemistry*
32 531 118:471–477. <https://doi.org/10.1111/j.1432-1033.1981.tb05543.x>
33 532 Reed CJ, Lewis H, Trejo E, et al (2013) Protein Adaptations in Archaeal Extremophiles.
34 533 *Archaea* 2013:1–14. <https://doi.org/10.1155/2013/373275>
35 534 Savitski MM, Reinhard FBM, Franken H, et al (2014) Tracking cancer drugs in living cells by
36 535 thermal profiling of the proteome. *Science* 346:1255784.
37 536 <https://doi.org/10.1126/science.1255784>
38 537 Shevack A, Gewitz HS, Hennemann B, et al (1985) Characterization and crystallization of
39 538 ribosomal particles from *Halobacterium marismortui*. *FEBS Letters* 184:68–71.
40 539 [https://doi.org/10.1016/0014-5793\(85\)80655-4](https://doi.org/10.1016/0014-5793(85)80655-4)
41 540 Singh S, Gupta M, Gupta Y (2020) Microbial Life at Extreme of Salt Concentration:
42 541 Adaptation Strategies. In: Singh RP, Manchanda G, Maurya IK, Wei Y (eds) *Microbial*
43 542 *Versatility in Varied Environments: Microbes in Sensitive Environments*. Springer,
44 543 Singapore, pp 35–49
45 544 Sridharan S, Günthner I, Becher I, et al (2019) Target Discovery Using Thermal Proteome
46 545 Profiling. In: Tao WA, Zhang Y (eds) *Mass Spectrometry-Based Chemical Proteomics*, 1st
47 546 edn. Wiley, pp 267–291
48 547 Tadeo X, López-Méndez B, Castaño D, et al (2009) Protein Stabilization and the Hofmeister
49 548 Effect: The Role of Hydrophobic Solvation. *Biophysical Journal* 97:2595–2603.
50 549 <https://doi.org/10.1016/j.bpj.2009.08.029>
51 550 Talon R, Coquelle N, Madern D, Girard E (2014) An experimental point of view on
52 551 hydration/solvation in halophilic proteins. *Front Microbiol* 5:.
53 552 <https://doi.org/10.3389/fmicb.2014.00066>

- 1
2
3 553 Tan BX, Brown CJ, Ferrer FJ, et al (2015) Assessing the Efficacy of Mdm2/Mdm4-Inhibiting
4 554 Stapled Peptides Using Cellular Thermal Shift Assays. *Scientific Reports* 5:12116.
5 555 <https://doi.org/10.1038/srep12116>
6 556 Tan CSH, Go KD, Bisteau X, et al (2018) Thermal proximity coaggregation for system-wide
7 557 profiling of protein complex dynamics in cells. *Science* 359:1170–1177.
8 558 <https://doi.org/10.1126/science.aan0346>
9 559 Tehei M, Franzetti B, Madern D, et al (2004) Adaptation to extreme environments:
10 560 macromolecular dynamics in bacteria compared in vivo by neutron scattering. *EMBO reports*
11 561 5:66–70. <https://doi.org/10.1038/sj.embor.7400049>
12 562 Tehei M, Madern D, Pfister C, Zaccai G (2001) Fast dynamics of halophilic malate
13 563 dehydrogenase and BSA measured by neutron scattering under various solvent conditions
14 564 influencing protein stability. *PNAS* 98:14356–14361. <https://doi.org/10.1073/pnas.251537298>
15 565 Thombre RS, Shinde VD, Oke RS, et al (2016) Biology and survival of extremely halophilic
16 566 archaeon *Haloarcula marismortui* RR12 isolated from Mumbai salterns, India in response to
17 567 salinity stress. *Sci Rep* 6:. <https://doi.org/10.1038/srep25642>
18 568 Tokunaga H, Ishibashi M, Arakawa T, Tokunaga M (2004) Highly efficient renaturation of
19 569 beta-lactamase isolated from moderately halophilic bacteria. *FEBS Lett* 558:7–12.
20 570 [https://doi.org/10.1016/S0014-5793\(03\)01508-4](https://doi.org/10.1016/S0014-5793(03)01508-4)
21 571 Vaublare P, Marty V, Fabiani E, et al (2015) Molecular adaptation and salt stress response of
22 572 *Halobacterium salinarum* cells revealed by neutron spectroscopy. *Extremophiles* 19:1099–
23 573 1107. <https://doi.org/10.1007/s00792-015-0782-x>
24 574 Vaublare P, Natali F, Kleman JP, et al (2020) Surviving salt fluctuations: stress and recovery
25 575 in *Halobacterium salinarum*, an extreme halophilic Archaeon. *Sci Rep* 10:1–10.
26 576 <https://doi.org/10.1038/s41598-020-59681-1>
27 577 Ventosa A, de la Haba RR, Sánchez-Porro C (2015) *Haloarcula*. In: *Bergey's Manual of*
28 578 *Systematics of Archaea and Bacteria*, 1st edn. Wiley
29 579 Wright DB, Banks DD, Lohman JR, et al (2002) The Effect of Salts on the Activity and
30 580 Stability of *Escherichia coli* and *Haloferax volcanii* Dihydrofolate Reductases. *Journal of*
31 581 *Molecular Biology* 323:327–344. [https://doi.org/10.1016/S0022-2836\(02\)00916-6](https://doi.org/10.1016/S0022-2836(02)00916-6)
32 582 Zaccai G (2020) Molecular dynamics in cells: A neutron view. *Biochimica et Biophysica*
33 583 *Acta (BBA) - General Subjects* 1864:129475. <https://doi.org/10.1016/j.bbagen.2019.129475>
34 584 Zaccai G (2013) Ecology of Protein Dynamics. *Current Physical Chemistry* 3:9–16.
35 585 <https://doi.org/10.2174/1877946811303010004>
36 586 Zaccai G, Bunick GJ, Eisenberg H (1986a) Denaturation of a halophilic enzyme monitored by
37 587 small-angle neutron scattering. *Journal of Molecular Biology* 192:155–157.
38 588 [https://doi.org/10.1016/0022-2836\(86\)90471-7](https://doi.org/10.1016/0022-2836(86)90471-7)
39 589 Zaccai G, Wachtel E, Eisenberg H (1986b) Solution structure of halophilic malate
40 590 dehydrogenase from small-angle neutron and X-ray scattering and ultracentrifugation. *Journal*
41 591 *of Molecular Biology* 190:97–106. [https://doi.org/10.1016/0022-2836\(86\)90078-1](https://doi.org/10.1016/0022-2836(86)90078-1)
42 592
43
44
45
46
47
48
49
50
51
52
53
54
55
56
57
58
59
60



A

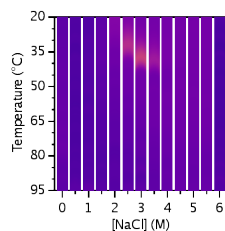
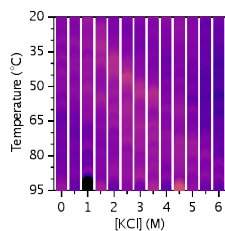
H. marismortui

Cell lysate

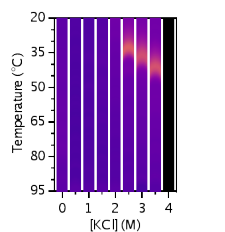
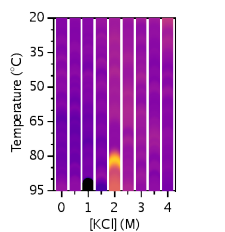
H. marismortui

MDH

NaCl



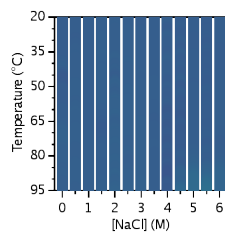
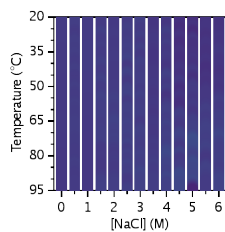
KCl



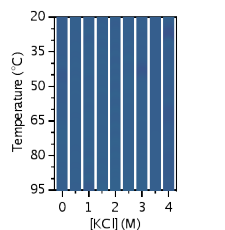
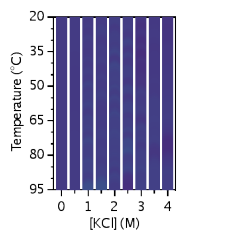
First derivative of ratio of
350/330nm fluorescence (°C⁻¹)

B

NaCl

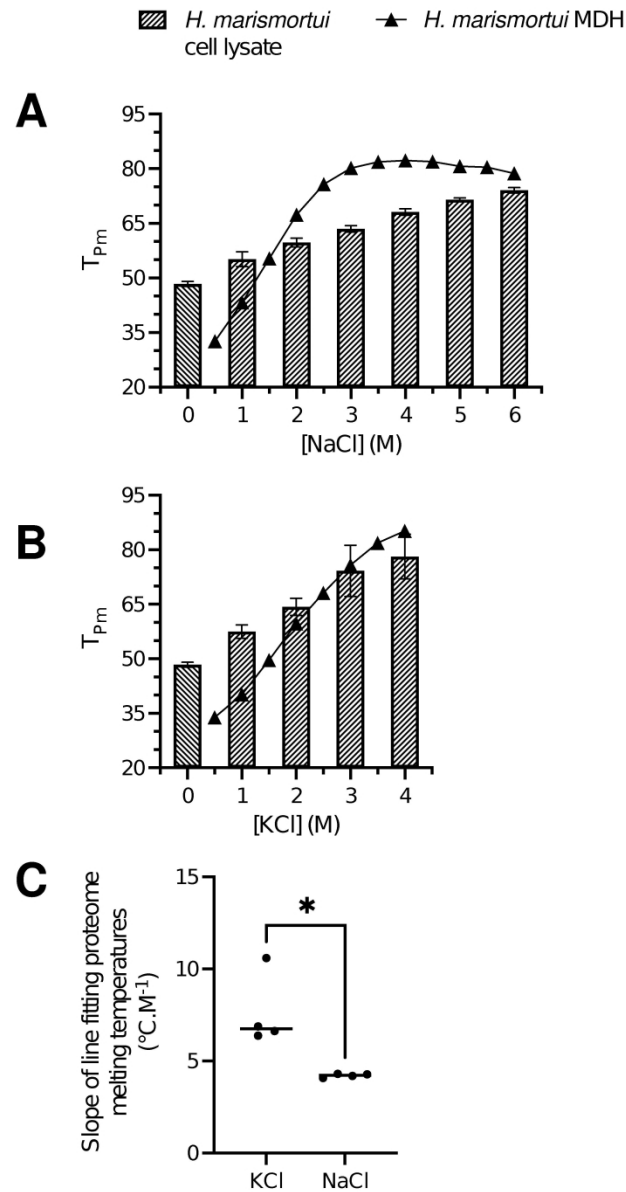


KCl



First derivative of light
scattering
(mAU·°C⁻¹)

1
2
3
4
5
6
7
8
9
10
11
12
13
14
15
16
17
18
19
20
21
22
23
24
25
26
27
28
29
30
31
32
33
34
35
36
37
38
39
40
41
42
43
44
45
46
47
48
49
50
51
52
53
54
55
56



45 Average values T_{Pm} defined as the temperature associated with maximum first derivative of 350/330nm
 46 fluorescence ratio measured with *H. marismortui* cell lysates under various concentrations of NaCl (A) and
 47 KCl (B) in 4 independent experiments. Abnormal high values at the end of the heating were excluded. Errors
 48 bars represent standard deviation. Melting temperatures of *H. marismortui* MDH, which were measured
 49 identically, are also given. For each independent experiment, linear regression of T_{Pm} as a function of NaCl
 50 and KCl concentration was made, as shown in Fig. S2b. Slopes of lines fitting the values are given and their
 51 difference is significant (*) according to a Mann-Whitney test ($P = 0.086$) (C).

52 118x219mm (600 x 600 DPI)

53
54
55
56
57
58
59
60

Fig. S1 Details of nanoDSF analysis of *H. marismortui* cell lysates

Values of 350 and 330nm fluorescence and their first derivatives, of 350/330 ratio and light scattering measured on soluble fractions of *H. marismortui* cells lysates upon a 20-95°C temperature increase at various NaCl and KCl concentrations. These data correspond to those presented in Fig. 1 ($OD_{600} = 1.104$).

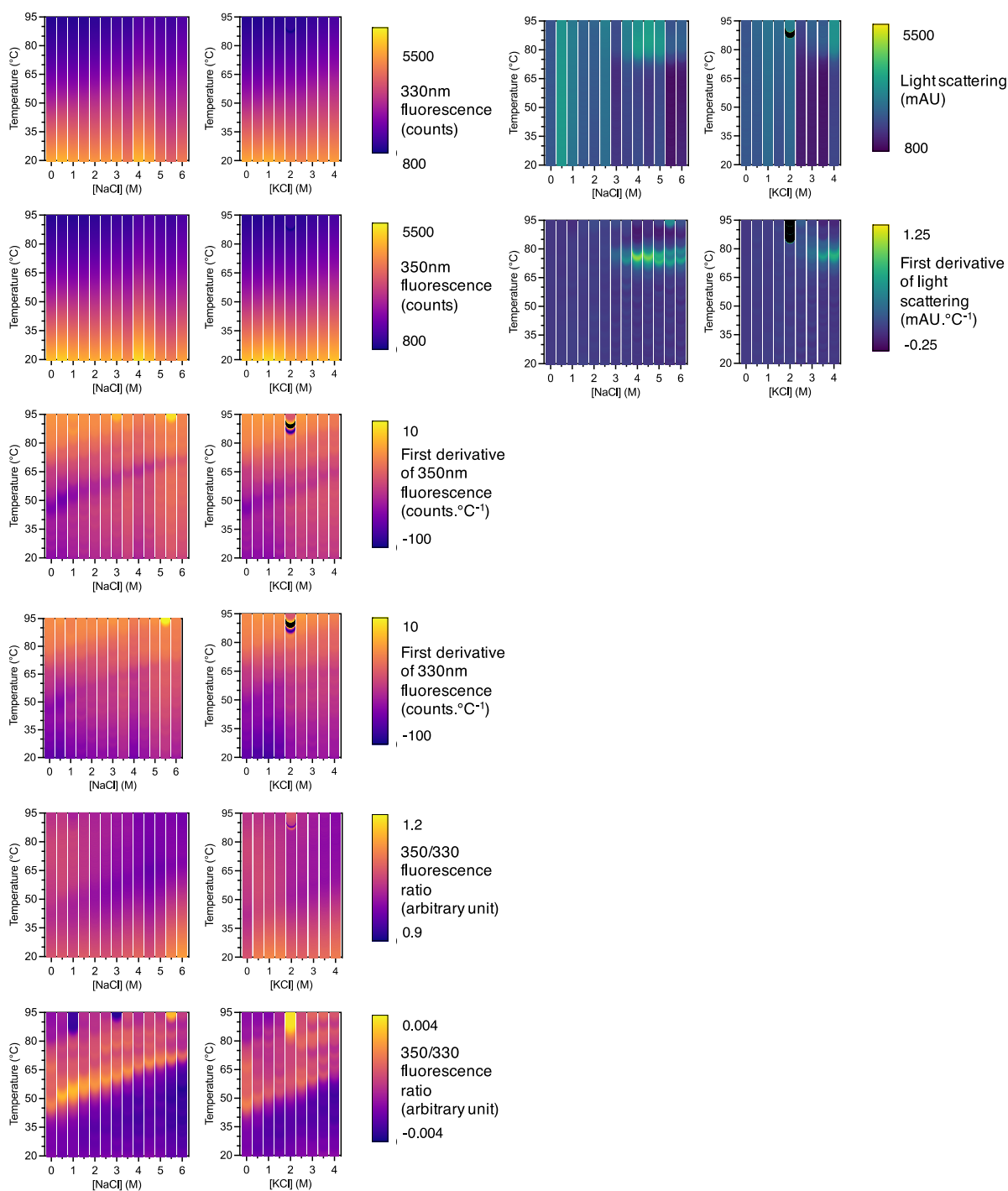


Fig. S2 Reproducibility of nanoDSF analysis of *H. marismortui* cell extracts

NanoDSF analysis of *H. marismortui* cells harvested at various OD₆₀₀ values (A) and values of proteome melting temperature (T_{Pm}), defined as the temperature associated with the peak of first derivative of ratio of 350/330nm fluorescence (B). Abnormal values occasionally happening close to the end of the experiment were excluded. Relation between salt concentration and T_{Pm} was fitted for each experiment with a linear regression. r^2 values are indicated. Data was obtained with larger steps in salt concentrations than in Fig. 1, except for the first column (DO 1.104) which was derived from this figure.

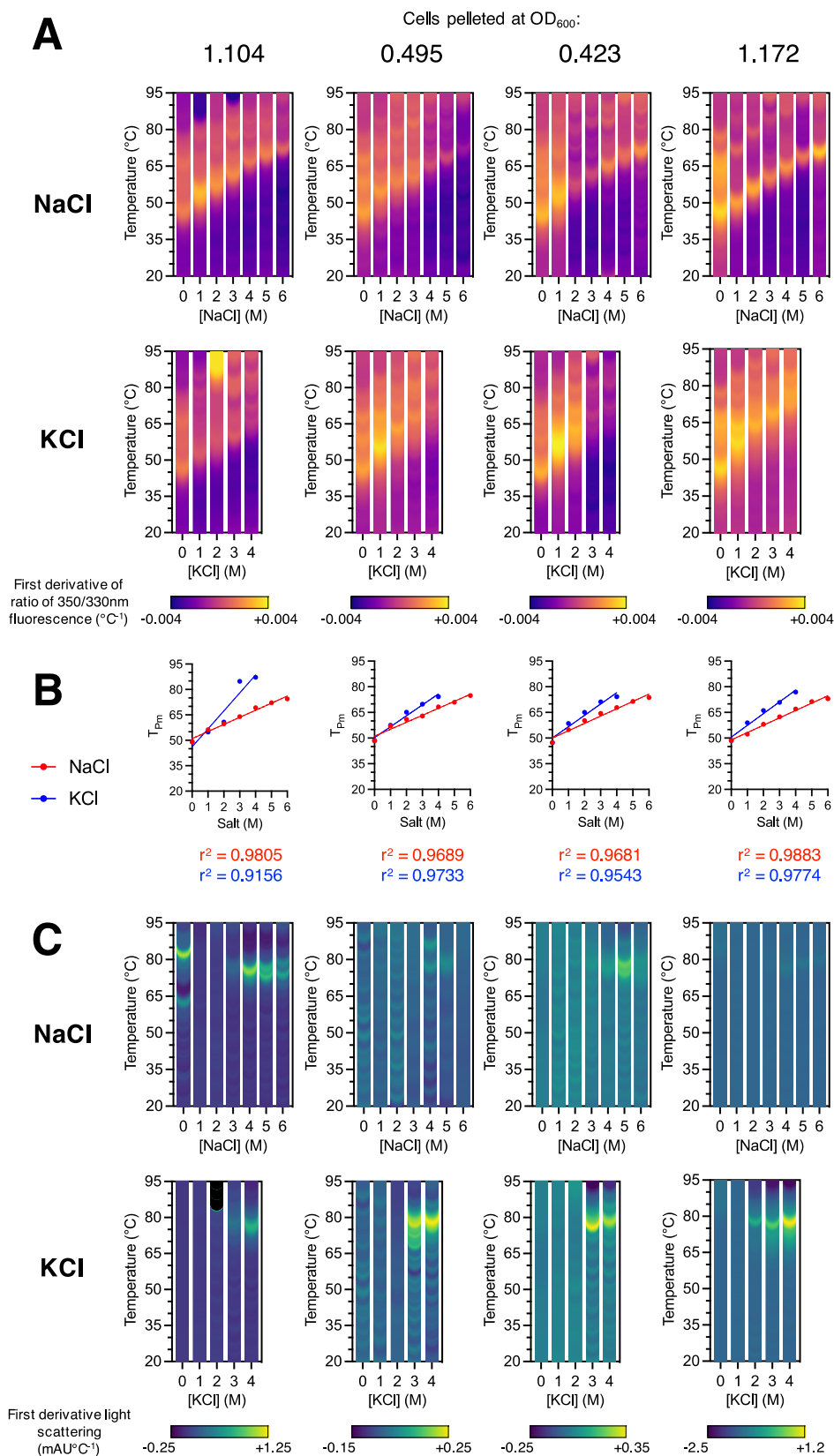


Fig. S2 Effect of dilution on thermal denaturation and aggregation curves of *H. marismortui* lysates

Final concentration of KCl was always 4M, only lysates were diluted.

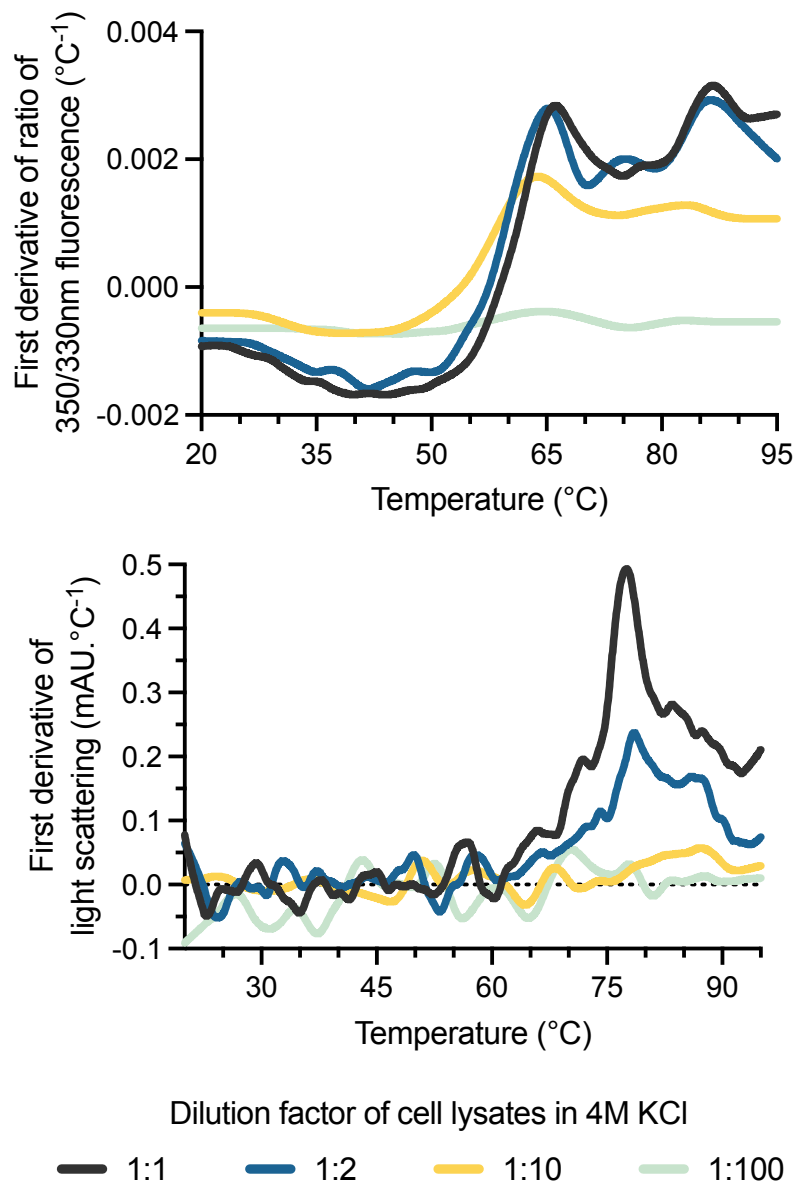


Fig. S4 nanoDSF analysis of *E. coli* cell lysates upon heating

NanoDSF analysis of cell lysates of non-halophilic *Escherichia coli* in various salt conditions. On the left, the color scales are the same than those used in Fig. 1 and Fig. 2. On the right a different color scale was used to improve contrast.

